UC San Diego
UC San Diego Previously Published Works

Title

The role of jet and film drops in controlling the mixing state of submicron sea spray aerosol particles

Permalink

https://escholarship.org/uc/item/3352q7tn

Journal

Proceedings of the National Academy of Sciences of the United States of America, 114(27)

ISSN

0027-8424

Authors

Wang, Xiaofei
Deane, Grant B
Moore, Kathryn A
et al.

Publication Date

2017-07-03

DOI

10.1073/pnas.1702420114

Peer reviewed

The role of jet and film drops in controlling the mixing state of submicron sea spray aerosol particles

Xiaofei Wang[a,1], Grant B. Deane[b,1], Kathryn A. Moore[a], Olivia S. Ryder[a], M. Dale Stokes[b], Charlotte M. Beall[b], Douglas B. Collins[a], Mitchell V. Santander[a], Susannah M. Burrows[c], Camille M. Sultana[a], and Kimberly A. Prather[a,b,2]

[a]Department of Chemistry and Biochemistry, University of California, San Diego, La Jolla, CA 92093; [b]Scripps Institution of Oceanography, University of California, San Diego, La Jolla, CA 92093; and [c]Atmospheric Science and Global Change Division, Pacific Northwest National Laboratory, Richland, WA 99354

The oceans represent a significant global source of atmospheric aerosols. Sea spray aerosol (SSA) particles comprise sea salts and organic species in varying proportions. In addition to size, the overall composition of SSA particles determines how effectively they can form cloud droplets and ice crystals. Thus, understanding the factors controlling SSA composition is critical to predicting aerosol impacts on clouds and climate. It is often assumed that submicrometer SSAs are mainly formed by film drops produced from bursting bubble-cap films, which become enriched with hydrophobic organic species contained within the sea surface microlayer. In contrast, jet drops formed from the base of bursting bubbles are postulated to mainly produce larger supermicrometer particles from bulk seawater, which comprises largely salts and water-soluble organic species. However, here we demonstrate that jet drops produce up to 43% of total submicrometer SSA number concentrations, and that the fraction of SSA produced by jet drops can be modulated by marine biological activity. We show that the chemical composition, organic volume fraction, and ice nucleating ability of submicrometer particles from jet drops differ from those formed from film drops. Thus, the chemical composition of a substantial fraction of submicrometer particles will not be controlled by the composition of the sea surface microlayer, a major assumption in previous studies. This finding has significant ramifications for understanding the factors controlling the mixing state of submicrometer SSA particles and must be taken into consideration when predicting SSA impacts on clouds and climate.

sea spray aerosol | mixing state | bubble bursting | jet drop | film drop

The oceans produce sea spray aerosol (SSA), one of the most abundant forms of atmospheric aerosol (1–3). It has been shown that individual SSA particles belong to one of several chemically distinct particle types (4). Knowledge of the type and amount of organic species in SSA is needed to predict concentrations of cloud condensation nuclei (CCN) and ice nuclei (IN) (5–8). The distribution of chemical species within and between SSA particles, generally referred to as aerosol mixing state, plays a critical role in affecting climate-relevant properties (9, 10). Because of the overall importance to climate, understanding the factors that control SSA mixing state is currently a major goal of many studies (4, 9, 10).

This study focuses on establishing a stronger foundation for the link between the physical production mechanisms and the chemical mixing state of submicrometer SSA particles. Here, a nascent SSA liquid drop produced at a relative humidity (RH) of 100% is called a "drop" and a dried (and therefore solid) drop is called a "particle." Particles from jet drops are called "jet drop particles" and particles from film drops are called "film drop particles." Most SSA particles are formed by bursting bubbles in whitecaps, which are produced by breaking waves (2, 11). There are two mechanisms that dominate the production of SSA in terms of number concentrations: (*i*) the bursting of a bubble-cap film, which produces film drops, and (*ii*) the fragmentation of a water jet formed during the collapse of the remaining cavity,

which produces jet drops. There is a third mechanism, which produces spume drops by the direct tearing of drops off wave crests at high wind speeds. Spume drops are large (from tens to hundreds of micrometers in scale) and thus quickly removed from the atmosphere by dry deposition (2). Given the critical importance of aerosol number concentration to marine cloud formation, in this study attention is limited to submicrometer SSA particle production from bubble bursting, which accounts for the largest number of SSA particles.

Due to differences in film and jet drop production, it has been implied that film and jet drops have vastly different compositions (5, 7). Film drops produced from bursting bubble-cap films become enriched with hydrophobic organics within the sea surface microlayer. In contrast, jet drops formed from the base of bursting bubbles are postulated to produce particles from bulk seawater, enriched largely in salts and water-soluble organic species. In both the analysis of observed SSA composition and the development of emission parameterizations of SSA for models, it is frequently assumed that submicrometer SSA particles are derived from film drops (2, 5, 12–16). Recent models that use the composition of SSA to predict specific cloud and climate properties have been greatly simplified by assuming all submicrometer SSAs are produced by the film drop production mechanism and directly reflect the composition of the sea surface microlayer (5, 6).

Significance

Submicrometer sea spray aerosol (SSA) particles play a critical role in determining cloud properties in marine environments. Typically, it is assumed that submicrometer SSA particles mainly originate from bubble-cap films bursting at the sea surface. However, we show that in addition to this formation pathway, a substantial fraction of submicrometer SSA particles are also produced from jet drops. Using an experimental approach that relies on differences in the electrical mobility of jet and film drops, we show that jet drops contribute up to 43% of total submicrometer SSA number concentrations. As shown herein, these two different production pathways result in an externally mixed submicrometer SSA population with two distinct chemical compositions with significantly different ice nucleating activities.

The assumption that jet drop particles do not contribute significantly to submicrometer SSA is based on the fact that extremely small bubbles (bubble radius $R_b < 20$ μm) are required to produce jet drop particles with diameter in the submicrometer range (2). Some studies have argued that bubbles of this size dissolve rapidly in the surrounding water before reaching the water surface (2, 17). However, there are a variety of bubble creation mechanisms which produce small bubbles directly at the sea surface, such as daughter bubble formation (18), and bubble dissolution does not limit their concentration at the surface during their short lifetime (18).

Moreover, it has been demonstrated that very small bubbles do produce jet drops. A recent study of bubbles bursting in fresh water reports a theoretical bubble size lower limit ($R_b = 4$ μm) for jet drop production (19), which is small enough to produce SSA in the submicrometer size range (2). Fresh water is considered to be a reliable proxy for bubble bursting in seawater because fresh water and seawater have similar surface tensions and viscosities (2, 20). This lower size limit for jet drop production from fresh water probably applies to seawater bubbles.

Thus, in contrast to the widely held assumption, it is possible that jet drop particles constitute a significant fraction of submicrometer SSA. However, there have been no detailed studies of the composition and properties of isolated jet drop particles produced from sub-100-μm bubbles ($R_b < 100$ μm). In this study, we present a method for determining the contribution of jet drop particles to the total submicrometer SSA number concentration in laboratory sea spray. Finally, we make a direct comparison of the size distributions, chemical compositions, and IN activities of submicrometer jet drop and film drop particles.

Results and Discussion

Jet Drop Particles Formed from Sub-100-μm Bursting Bubbles. Here we show that sub-100-μm bubbles produce a predictable population of jet drops whose sizes are related to their parent bubble sizes. A distribution of hydrogen bubbles with a mean radius in the range of 20–40 μm was produced through the electrolysis of seawater (see *SI Appendix, SI Methods* and Figs. S1 and S2A). This method provides precise control of bubble flux by adjustment of the current through the electrodes. The results of the experiments are shown in Fig. 1. The measured and modeled SSA particle production flux are plotted as a function of SSA particle diameter and the inset shows the measured and log-normal fitted electrolysis bubble flux plotted versus bubble radius (the production rate of hydrogen bubbles was determined using stoichiometry based on the measured electrode current). The modeled SSA particle flux was calculated from the electrolysis bubble flux using the 10% rule combined with the additional assumption that each electrolysis bubble produces exactly one drop. The so-called "10% rule" asserts that the diameter of the top jet drop produced by a bursting bubble, measured at an RH of 80%, is ~10% of the bubble radius (2). Dry SSA particle diameter (D_p) is ~1/2 of its value at an RH of 80% (2), therefore it follows that $D_p = 0.05R_b$.

The satisfactory fit and absolute numerical reconciliation between the observed and predicted particle production flux support the conclusion that the larger particle mode ($D_p > 1$ μm) observed in the electrolysis experiments consisted of jet drop particles. However, the 10% rule significantly underestimates the production of particles in the submicrometer size range, which may have been produced as secondary or tertiary drops in a series of jet drops, or alternatively through another mechanism, such as small satellite drops formed in between large primary jet drops (2).

Bursting bubble-cap films can be ruled out as the source of these particles through the following arguments. First, experimental studies have shown that bubbles with $R_b < 500$ μm do not produce film drops when they burst (2, 12, 21–23). Second, even assuming bursting bubbles in the electrolysis experiment size range—on the order of 10–100-μm radius—can produce film drops, our theoretical calculations indicate that such film drop
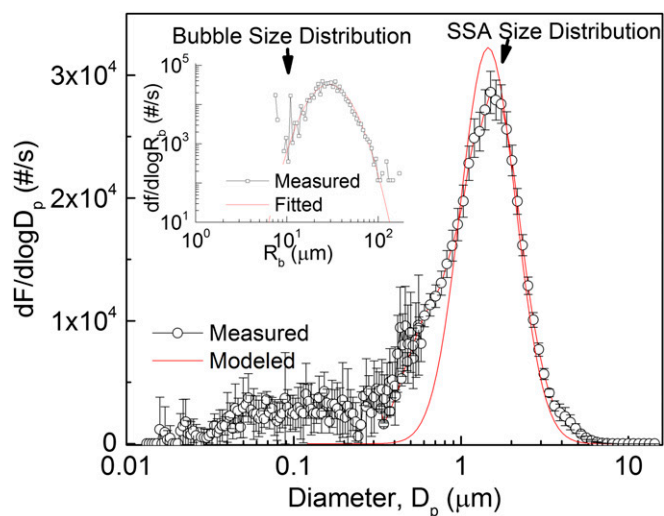

Fig. 1. Submicrometer jet drop particle production from electrolysis bubbles: measured (black circles) and calculated (red line) SSA particle size distributions. The size distributions were measured with a scanning mobility particle sizer and an aerodynamic particle sizer. (*Inset*) Observed (black squares) and fitted (red line) electrolysis bubble size distributions. dF/dlogD_p and df/dlogR_b are production fluxes (number of particles/bubbles per second) of submicrometer SSA particles and sub-100-μm bubbles, respectively. Error bars represent 1 SD.

particles must be less than 0.1-μm dry diameter (see *SI Appendix, SI Methods*), which cannot account for the majority of the particles shown in Fig. 1.

The electrolysis experiments challenge the widely held assumption that most submicrometer SSA particles come from film drops. If breaking ocean waves generate sufficiently high concentrations of sub-100-μm bubbles that burst on the sea surface, generated jet drops could contribute significantly to submicrometer SSA particles. Indirect evidence for the formation of bubbles in the required size range is provided by the observation that breaking waves radiate underwater noise up to 250 kHz (24), associated with the formation of bubbles of radius 13 μm (25).

Previous studies of SSA produced using a weir or a frit with a very fine pore size have reported SSA production from sub-100-μm bubbles (16, 26). Unlike electrolysis, these methods also generate bubbles with $R_b > 500$ μm, which can produce significant numbers of submicrometer film drops. For example, a bubble with $R_b = 1,000$ μm can produce more than 100 film drops (21), and indeed, these studies have reported a dominant particle mode that peaked at about 100-nm dry diameter, which was attributed to film drop particles. Sellegri et al. found another aerosol mode that peaks at ~300 nm in addition to the dominant 100-nm film drop particle mode (16). The presence of this larger 300-nm aerosol mode was attributed to the impaction of film drops onto other film caps, forcefully breaking the film and leading to the formation of larger film drops. However, our findings suggest that this larger aerosol mode may be simply due to the jet drop production from bursting of the sub-100-μm bubbles.

Significant Contributions of Jet Drops to Submicrometer SSA from a Breaking Wave Analog. Motivated by the discovery that submicrometer SSA can be produced from jet drops, we conducted a series of experiments to quantify the relative contributions of jet and film drops to total submicrometer SSA.

We developed a technique for discriminating between jet and film drops based on their differences in electrical mobility. It is well known that SSA particles are electrically charged, and that the charge distribution of jet drops and film drops differ, with jet drops often carrying more electrical charge than film drops (11, 14). This

difference can be used to distinguish jet and film drops by measuring each drop's electrical mobility (denoted Z_p), which is a function of the ratio of particle charge to diameter (*SI Appendix, SI Methods*). We measured the electrical mobility distributions (EMDs) of positively and negatively charged submicrometer particles (EMD⁺, EMD⁻) in populations of jet drops produced from sub-100-μm radius bubbles and film drops produced from 0.6–2-mm-radius bubbles.

Jet drops from electrolysis bubbles are not suitable for EMD analysis because of the potential for electrolysis to alter the electrical mobility of SSA particles. A "nucleation bubbler," which produces bubbles ~15 μm in radius (*SI Appendix*, Figs. S2*B* and S3), was developed as an alternative to electrolysis for producing jet drops (*SI Appendix, SI Methods* and Fig. S1). Any supermicrometer particles produced by the nucleation bubbles were removed using an in-line impactor with a size cut at 0.8 μm. As the measured size distribution shows (*SI Appendix*, Fig. S3), the nucleation bubbles produced SSA particles in the submicrometer size range that were consistent with the electrolysis experiments and previous calculations showing that bubbles larger than 4-μm radius in water will produce jet drops (19).

Film drops were produced from 0.6–2-mm radius bubbles generated with a glass frit (*SI Appendix, SI Methods* and Figs. S1 and S4), as bubbles in this size range are known to produce predominately film drops (2). The size distribution of SSA particles from the film drops is shown in *SI Appendix*, Fig. S4*C*. According to the 10% rule, SSA particles from jet drops produced by 0.6–2-mm-radius bubbles have diameters ranging from ~30–100 μm, which were removed from the SSA by the same in-line impactor used for the nucleation bubble SSA analysis.

The positive and negative EMDs for submicrometer SSA particles from film drops are shown in Fig. 2*A*. The two EMDs have similar shapes and magnitudes (EMD⁺ ~ EMD⁻ for submicrometer film drop particles). In contrast, the EMDs of negatively and positively charged submicrometer jet drop particles (Fig. 2*B*) are distinct (EMD⁺ ≠ EMD⁻ for submicrometer jet

drop particles). Additionally, submicrometer jet drop particles tend to have higher electrical mobilities than film drop particles. Interestingly, as shown in *SI Appendix*, Fig. S5, the organic species present in seawater significantly alter the shapes of the EMDs of submicrometer jet drop particles (but not film drop particles) and also the relative abundance of negatively and positively charged jet drop particles.

We have quantified the relative abundance of jet drop and film drop particles when produced by a source that generates both drop types simultaneously. The source consisted of an intermittent plunging water sheet in a marine aerosol reference tank (MART), which serves as a proxy for a breaking wave (27). The particle size distribution of submicrometer SSA from the MART is shown in *SI Appendix*, Fig. S6, which does not show any obvious evidence of distinct film drop and jet drop modes. To separate out the production modes, we have used the differences between film and jet drop particle EMDs. Fig. 2*C* shows the EMD⁺ and EMD⁻ of submicrometer SSA from a typical MART experiment. The positive and negative EMDs each contain two log-normal modes, respectively designated POS1, POS2 in EMD⁺, and NEG1, NEG2 in EMD⁻ (Fig. 2*C*).

The mode amplitudes, means, and SDs were estimated for POS1, POS2 and NEG1, NEG2 using a least-mean-squares, log-normal mode fit to the positive and negative EMDs (Fig. 2*D*). Note that the EMDs of jet drop particles from the nucleation bubbles may contain more than one log-normal mode (Fig. 2*B*). It is important to note that the nucleation bubbler is an artificial source of jet drops that was convenient to unambiguously illustrate the differences in electrical mobility between jet and film drops, but is not representative of wave breaking. Our final analysis of electrical mobility (Fig. 2 *C* and *D*) was used to determine the relative contributions of jet versus film drops in natural SSA. Submicrometer SSA was generated by a plunging waterfall in an MART, which has been calibrated against actual laboratory breaking waves and determined to be a good proxy for
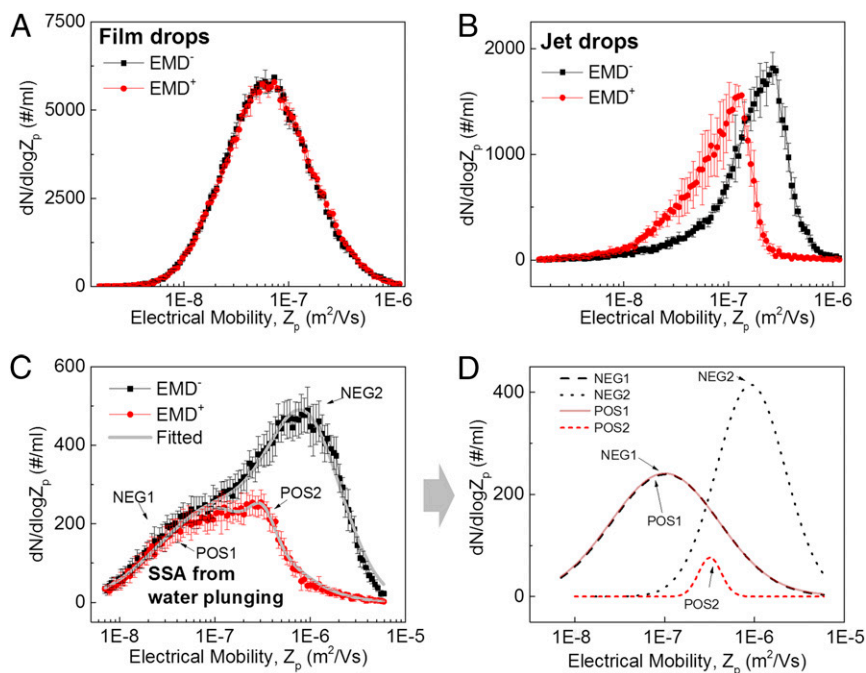
Fig. 2. Contribution of jet drops to submicrometer SSA particles: EMDs of negatively (EMD⁻, black squares) and positively (EMD⁺, red dots) charged submicrometer particles. (*A*) Film drop particles produced from frit-sized (0.6~2-mm radius) bubbles in natural seawater. (*B*) Jet drop particles produced from sub-100-μm nucleation bubbles in natural seawater. (*C*) Electrical mobility distributions of negatively (EMD⁻) and positively (EMD⁺) charged submicrometer SSA produced from a plunging waterfall in an MART. The gray lines are fitted results (sum of POS1 + POS2 and sum of NEG1 + NEG2). (*D*) Results of peak fitting for the curves (EMD⁻ and EMD⁺) shown in *C*. Error bars represent the SD of the data.

the physical and chemical properties of sea spray from a breaking wave (27). We find that the EMDs from the mixed population of film and jet drop particles generated by the MART are fit well using four log-normal modes (two for the EMD$^+$ and two for the EMD$^-$) with a very low residual. That is, the EMD distributions relevant to the ocean are well-represented by log-normal modes.

We performed a decomposition (*SI Appendix*, Fig. S7) of the EMDs shown in Fig. 2C from the MART source with six log-normal modes (three for the EMD$^+$ and three for the EMD$^-$) to see if adding an additional mode significantly affected the analysis. We found an insignificant shift (1%) in our final estimate of jet versus film drops (described below), confirming that two log-normal modes for each EMD were sufficient.

The log-normal mode fits to the EMDs can be interpreted in terms of jet and film drop production. The left tails (for $\bar{Z}_p < {\sim}3 \times 10^{-7}$ m^{2}V^{-1}·s^{-1}) of EMD$^+$ and EMD$^-$ overlay, and consequently the POS1 and NEG1 modes have the same shape and magnitude. Symmetric positive and negative distributions are consistent with the EMDs of film drop particles. In contrast, the shape and amplitude of the POS2 and NEG2 modes differ, consistent with the asymmetric EMDs of jet drop particles (Fig. 2B). The fact that the POS1 and NEG1 modes have lower electrical mobilities than the POS2 and NEG2 modes is also consistent with the conclusion that POS1 and NEG1 consist of film drop particles whereas POS2 and NEG2 are jet drop particles. Fig. 2 A and B shows that the EMDs of jet drop particles peak at a higher electrical mobility than the EMDs of film drop particles.

The fraction of SSA consisting of jet drop particles was estimated from the fitted EMD modes. The integral of POS2 and NEG2 yields the number concentration of jet drop particles. Dividing the estimated jet drop particle concentration by the total SSA submicrometer particle concentration (measured with a scanning mobility particle sizer—*SI Appendix, SI Methods*) yields an estimate for the fraction of SSA produced by the jet drop production mechanism.

To investigate the effect of seawater biological conditions on SSA production mechanisms, a phytoplankton bloom was induced in natural seawater in an MART (*SI Appendix, SI Methods*). *SI Appendix*, Fig. S8A shows chlorophyll-a concentrations during the experiment, indicating the progression of the bloom. Eight EMDs (1 per day) were measured over the course of the experiment (*SI Appendix*, Fig. S8B), and were used to calculate the contributions of jet drop production to total submicrometer SSA concentrations.

We note that a significant fraction of SSA can be attributed to jet drops, the estimate ranging from a low of ~20% in natural seawater, increasing over the course of the bloom to a high of ~43%. The systematic increase in the fraction of jet drops occurred during the bloom growth phase and remained high but variable after the peak in chlorophyll-a concentrations (*SI Appendix*, Figs. S8A and S9). Given the time-dependent nature of the fraction of jet drop particles in SSA observed over the course of the phytoplankton bloom, we conclude that changes in seawater chemistry affected the production mechanism and hence the relative proportion of submicrometer SSA particles produced by jet versus film drops (28). This represents a major finding, demonstrating that oceanic biological conditions can influence the mechanisms producing SSA.

Major Differences in the Compositions of Submicrometer Film and Jet Drop Particles. Because a significant fraction of SSA is produced by the jet drop mechanism (up to 43% depending on seawater chemistry), it is important to understand the differences in chemical composition and climate-relevant properties of SSA particles produced by these two production pathways from natural seawater. Because there is currently no way to physically separate film and jet drop particles in an MART, we have based our measurements on the same film and jet drop sources used to study the EMDs: Submicrometer film drop particles were produced by

the glass frit whereas submicrometer jet drop particles were produced by the nucleation bubbler (*SI Appendix, SI Methods*).

The chemical compositions of submicrometer film and jet drop particles were characterized with a high-resolution aerosol mass spectrometer (*SI Appendix*). The organic species in the mass spectra of submicrometer particles produced by film and jet drop particles are clearly distinct (Fig. 3 A and C): Film drop particles contain a higher fraction of aliphatic (i.e., hydrophobic) organic species (Fig. 3A), whereas jet drop particles contain a larger fraction of oxygen-containing (i.e., more water-soluble) organic species (Fig. 3C). This is consistent with our previous study, which also shows that the organic species in super-micrometer SSA have higher oxygen-to-carbon ratios (13).

The morphologies of film and jet drop particles and their organic volume fractions were measured by atomic force microscopy (AFM) (*SI Appendix, SI Methods*). In this set of experiments, the frit and nucleation bubbler were run simultaneously in the same volume of seawater (*SI Appendix*, Fig. S1E). Particles were collected on silicon wafer chips using a Micro-Orifice Uniform Deposit Impactor (MOUDI). This experimental design rules out any possible effect of different organic depletion rates in the two bubbler systems (bubbles from the nucleation bubbler collectively have a much smaller gas flow rate than bubbles from the frit). Film drop particles from large bubbles and jet drop particles from nucleation bubbles were differentiated based upon dry particle sizes (*SI Appendix*, Fig. S10). Fig. 3 B and D shows typical AFM phase images of representative film and jet drop particles. Both particles have a core–shell structure typical of dry SSA particles: a salt core and an organic-rich shell. The organic volume fraction was determined by analyzing AFM phase and topography images (29). Fig. 3E shows the organic volume fraction for individual SSA film and jet drop particles. The separation between the organic volume fractions of the two populations illustrates that the organic contribution to jet drop particles from nucleation bubbles is significantly smaller than that in film drop particles produced by frit bubbles.

The question exists as to how the observed differences in composition between jet and film drop particles impact the cloud-relevant properties of SSA. Recent studies report that SSA particles can be a major source of ice nucleating particles (INPs) in the marine atmosphere (7, 30, 31). Fig. 3F shows the temperature-dependent fraction of INPs in film and jet drop populations produced from natural seawater (*SI Appendix*). We have shown that submicrometer jet drop particles have much higher INP activities and freeze at much warmer temperatures than film drop particles.

It is important to note that the size distribution of jet drop particles studied here is significantly different from that of the film drop particles (*SI Appendix*, Figs. S3 and S4). Thus, the observed differences in INP activity could possibly be explained by the increase in either total surface area or volume associated with jet drop particle populations. If the IN active entities are transported on the drop surface, then one would expect their presence within drops to scale with the surface area of the drop population. If carried within the drop liquid core, then the IN active entities should scale with the volume of the drop population. Surface area and volume scaling laws have been applied to the film drop INP activity curve in Fig. 2F. Neither scaled curve approaches the jet drop INP activity curve (*SI Appendix*, Fig. S11), implying some concentration mechanism for INP active substances during jet drop production well beyond anything that can be explained by simple surface area or volume scaling of the smaller film drops.

Atmospheric Implications. The jet versus film drop laboratory experiments have a number of climate-relevant consequences for aerosol modeling: (*i*) a significant fraction of submicrometer SSAs is composed of jet drop particles (20~43%); (*ii*) the fraction of jet drops depends on seawater chemistry and changes over the course of a phytoplankton bloom; (*iii*) the chemical compositions of jet and film drop particles are distinct and introduce selective pathways
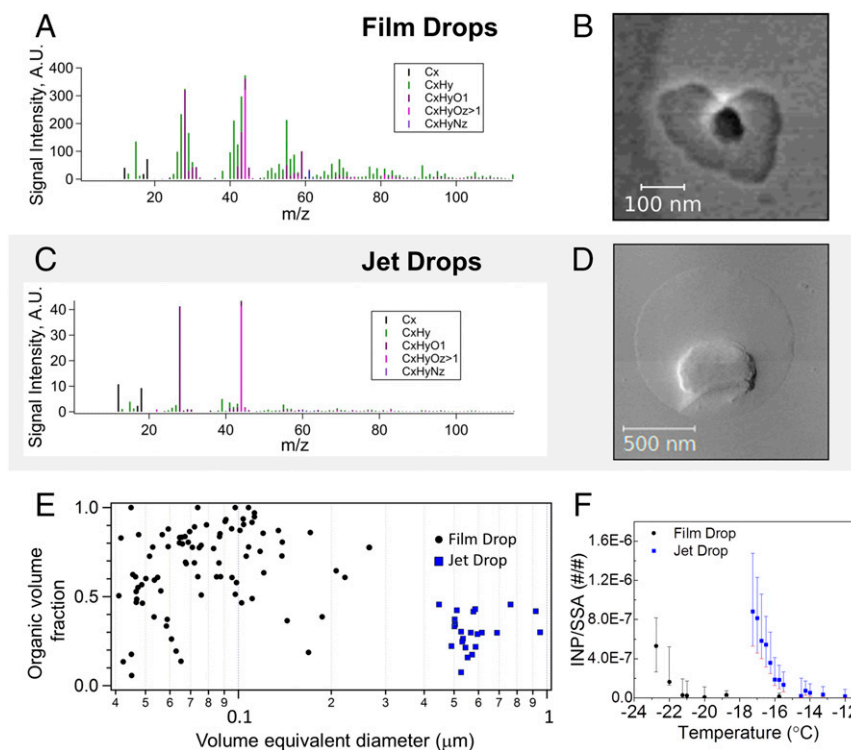
Fig. 3. Differences in chemical composition between submicrometer film drop and jet drop particles: AMS mass spectra for submicrometer (*A*) film and (*C*) jet drop particles. Typical AFM phase images for submicrometer (*B*) film drop particles and (*D*) jet drop particles. (Scale bars: *B*, 100 nm long; *D*, 500 nm long.) (*E*) Organic volume fractions for submicrometer particles produced by film and jet drops (determined from AFM images). (*F*) Number fraction of INPs in film and jet drop particles. Error bars represent 1 SD.

for the transport of soluble (jet) and insoluble (film) organic species; and (*iv*) composition differences result in jet drop particles being more IN active at warmer temperatures than film drop particles.

Differences in the organic composition and the organic/salt ratio of jet and film drop particles result in externally mixed populations of submicrometer SSA (Fig. 4). Film drops transport aliphatic-rich hydrophobic organic species concentrated in the sea surface microlayer and jet drops transport more soluble organic species with higher oxygen/carbon ratios from the underlying seawater (5, 13). A quantitative understanding of these distinct transport pathways for organic species will allow their impacts on aerosol chemistry to be included in models that calculate the organic fraction of submicrometer SSA and the associated climate-relevant properties, such as INP and CCN activities. For example, in a recent study of marine IN aerosols, Wilson et al. assume that the relative number of ice nucleating entities (INE) per gram of total organic carbon is the same in the aerosol phase and the sea surface microlayer (7). Our results suggest that this assumption will only be valid for a limited fraction of submicrometer SSA particles.

The IN characterization study of jet drop particles shows that the jet drop production of SSA is a more efficient transport pathway for INEs. There are several plausible reasons that can account for this. Organic particles may be adsorbed onto the boundary of a bubble as it rises through the seawater. Boundary layer flow around the rising bubble may concentrate particulate INEs at the base of the bubble. Because jet drops are made from the water at the base of a bubble (2), they may be enriched in INEs compared with film drops because of this scavenging and concentration process.

Variation in the fraction of jet drop particles observed over the course of a phytoplankton bloom shows that environmental factors

(e.g., seawater chemistry; *SI Appendix*, Fig. S9) can significantly alter the contribution of jet drops to the total submicrometer SSA population. Because film and jet drop production mechanisms provide distinct and selective transport pathways for organic species with different properties, modulation of their relative contributions could drive the mixing state of SSA, with
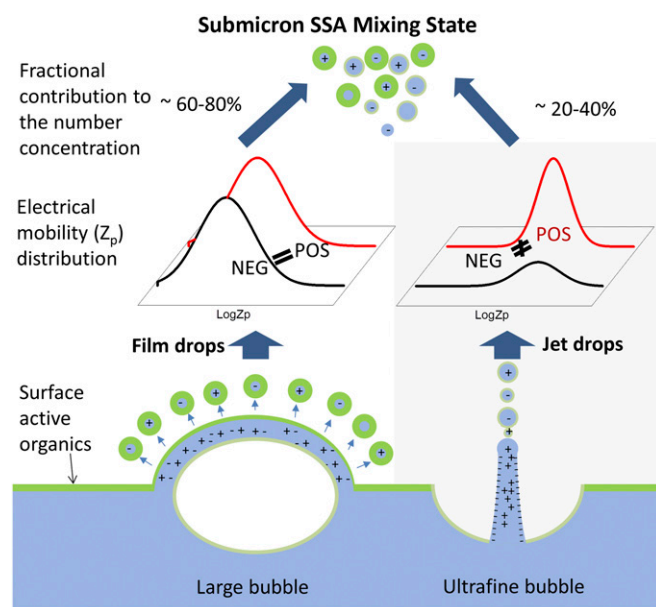

Fig. 4. Schematic diagram linking the origin of the submicrometer SSA mixing state to film and jet drop production mechanisms.

important implications for the concentration of CCN and IN in the marine boundary layer (9, 10).

Finally, we note that many previous SSA studies used frit bubblers to produce SSA (15, 16, 32). Our findings suggest that studies of SSA from frits will lack an important component of jet drop particles produced by sub-100-μm bubble bursting. Continuous bubbling through a frit can generate a persistent layer of foam to which sub-100-μm bubbles may be lost through coalescence. For example, a widely used SSA production flux parameterization (15) is based upon experiments using a glass frit for bubble generation. Thus, climate models using SSA parameterizations obtained from frit experiments will miss the contribution of jet drop particles to submicrometer SSA, leading to errors in SSA number flux and chemical composition.

Methods

Definition Used for SSA Size. SSA size changes with RH. In this study, SSA particles were dried (RH < 20%) before any measurement. Thus, all sizes reported in this paper are SSA dry diameter (D_p) in nanometers or micrometers. A commonly used set of relations for particle size is

$$D_p = 0.5D_{80\%} = r_{80\%} = 0.25D_{drop} = 0.5r_{drop},$$

where D is particle diameter, r is particle radius, and the subscripts p, 80%, and $drop$ mean equilibrium size at RH <20%, 80%, and 100%, respectively.

SSA Production and Characterization. In this study, submicrometer SSA particles were produced through a variety of methods for different purposes. Isolated jet drop particles were produced via bursting of sub-100-μm bubbles generated from either electrolysis of seawater or bubble nucleation. Isolated film drop particles were produced via bursting of 0.6–2-mm-radius bubbles generated from a glass frit. Natural SSA, a mixture of jet drop and film drop particles, was produced using an intermittent plunging water sheet in an MART, which serves as a proxy for a breaking wave (27). The physical and chemical properties of SSA particles were characterized. The electrical mobility distributions of SSA were measured using a differential mobility analyzer followed by a condensational particle counter. Their size distributions were measured with a scanning mobility particle sizer and an aerodynamic particle sizer, whereas organic compositions were measured using an aerosol mass spectrometer (AMS). Particle morphology and organic volume fractions were derived using AFM, and IN activities were measured using an automatic ice spectrometer. More detailed descriptions of these techniques and their data analysis procedures can be found in *SI Appendix*.

1. de Leeuw G, et al. (2011) Production flux of sea spray aerosol. *Rev Geophys* 49:RG2001.
2. Lewis ER, Schwartz SE (2004) *Sea Salt Aerosol Production: Mechanisms, Methods, Measurements and Models—A Critical Review* (American Geophysical Union, Washington, DC).
3. O'Dowd CD, de Leeuw G (2007) Marine aerosol production: A review of the current knowledge. *Philos Trans A Math Phys Eng Sci* 365:1753–1774.
4. Prather KA, et al. (2013) Bringing the ocean into the laboratory to probe the chemical complexity of sea spray aerosol. *Proc Natl Acad Sci USA* 110:7550–7555.
5. Burrows SM, et al. (2014) A physically based framework for modeling the organic fractionation of sea spray aerosol from bubble film Langmuir equilibria. *Atmos Chem Phys* 14:13601–13629.
6. McCoy DT, et al. (2015) Natural aerosols explain seasonal and spatial patterns of Southern Ocean cloud albedo. *Sci Adv* 1:e1500157.
7. Wilson TW, et al. (2015) A marine biogenic source of atmospheric ice-nucleating particles. *Nature* 525:234–238.
8. Burrows SM, Hoose C, Pöschl U, Lawrence MG (2013) Ice nuclei in marine air: Biogenic particles or dust? *Atmos Chem Phys* 13:245–267.
9. Schill SR, et al. (2015) The impact of aerosol particle mixing state on the hygroscopicity of sea spray aerosol. *ACS Cent Sci* 1:132–141.
10. Collins DB, et al. (2013) Impact of marine biogeochemistry on the chemical mixing state and cloud forming ability of nascent sea spray aerosol. *J Geophys Res Atmos* 118:8553–8565.
11. Blanchard DC (1963) The electrification of the atmosphere by particles from bubbles in the sea. *Prog Oceanogr* 1:73–202.
12. Veron F (2015) Ocean spray. *Annu Rev Fluid Mech* 47:507–538.
13. Wang X, et al. (2015) Microbial control of sea spray aerosol composition: A tale of two blooms. *ACS Cent Sci* 1:124–131.
14. Woolf DK, Bowyer PA, Monahan EC (1987) Discriminating between the film drops and jet drops produced by a simulated whitecap. *J Geophys Res Oceans* 92:5142–5150.
15. Mårtensson EM, Nilsson ED, de Leeuw G, Cohen LH, Hansson HC (2003) Laboratory simulations and parameterization of the primary marine aerosol production. *J Geophys Res Atmos* 108:4297.
16. Sellegri K, O'Dowd CD, Yoon YJ, Jennings SG, de Leeuw G (2006) Surfactants and submicron sea spray generation. *J Geophys Res Atmos* 111:D22215.
17. Blanchard DC, Woodcock AH (1957) Bubble formation and modification in the sea and its meteorological significance. *Tellus* 9:145–158.
18. Bird JC, de Ruiter R, Courbin L, Stone HA (2010) Daughter bubble cascades produced by folding of ruptured thin films. *Nature* 465:759–762.
19. Lee JS, et al. (2011) Size limits the formation of liquid jets during bubble bursting. *Nat Commun* 2:367.
20. Lhuissier H, Villermaux E (2012) Bursting bubble aerosols. *J Fluid Mech* 696:5–44.
21. Blanchard DC, Syzdek LD (1988) Film drop production as a function of bubble size. *J Geophys Res Oceans* 93:3649–3654.
22. Resch F, Afeti G (1991) Film drop distributions from bubbles bursting in seawater. *J Geophys Res Oceans* 96:10681–10688.
23. Wu J (1994) Film drops produced by air bubbles bursting at the surface of seawater. *J Geophys Res Oceans* 99:16403–16407.
24. Dahl PH, Jessup AT (1995) On bubble clouds produced by breaking waves: An event analysis of ocean acoustic measurements. *J Geophys Res Oceans* 100:5007–5020.
25. Deane GB, Stokes MD (2010) Model calculations of the underwater noise of breaking waves and comparison with experiment. *J Acoust Soc Am* 127:3394–3410.
26. Fuentes E, Coe H, Green D, de Leeuw G, McFiggans G (2010) Laboratory-generated primary marine aerosol via bubble-bursting and atomization. *Atmos Meas Tech* 3:141–162.
27. Stokes MD, et al. (2013) A marine aerosol reference tank system as a breaking wave analogue for the production of foam and sea-spray aerosols. *Atmos Meas Tech* 6:1085–1094.
28. Stokes MD, et al. (2016) A miniature marine aerosol reference tank (mini-MART) as a compact breaking wave analogue. *Atmos Meas Tech* 9:4257–4267.
29. Ryder OS, et al. (2015) Role of organic coatings in regulating N_2O_5 reactive uptake to sea spray aerosol. *J Phys Chem A* 119:11683–11692.
30. DeMott PJ, et al. (2016) Sea spray aerosol as a unique source of ice nucleating particles. *Proc Natl Acad Sci USA* 113:5797–5803.
31. McCluskey CS, et al. (2017) A dynamic link between ice nucleating particles released in nascent sea spray aerosol and oceanic biological activity during two mesocosm experiments. *J Atmos Sci* 74:151–166.
32. Long MS, et al. (2014) Light-enhanced primary marine aerosol production from biologically productive seawater. *Geophys Res Lett* 41:2661–2670.

EARTH, ATMOSPHERIC, AND PLANETARY SCIENCES